



Published in final edited form as:

J Cardiovasc Electrophysiol. 2012 December ; 23(12): 1364–1371. doi:10.1111/j.1540-8167.2012.02400.x.

Intracellular Calcium Dynamics, Shortened Action Potential Duration and Late-phase 3 Early Afterdepolarization in Langendorff-Perfused Rabbit Ventricles

Liang Tang, PhD¹, Boyoung Joung, MD, PhD², Masahiro Ogawa, MD, PhD², Peng-Sheng Chen, MD², and Shien-Fong Lin, PhD²

¹Department of Biomedical Engineering, University of Texas at San Antonio, San Antonio, TX 78249

²Krannert Institute of Cardiology, Department of Medicine, Indiana University School of Medicine, Indianapolis, IN 46202

Abstract

Introduction—To elucidate the mechanism of late-phase 3 early after depolarization (EAD) in ventricular arrhythmogenesis, we hypothesized that intracellular calcium (Ca_i) overloading and action potential duration (APD) shortening may promote late phase 3 EAD and triggered activity, leading to development of ventricular fibrillation (VF).

Methods and Results—In isolated rabbit hearts, we performed microelectrode recording and simultaneous dual optical mapping of transmembrane potential (V_m) and Ca_i transient on left ventricular endocardium. An I_{KATP} channel opener, pinacidil, was used to abbreviate action potential duration (APD). Rapid-pacing was then performed. Upon abrupt cessation of rapid pacing with cycle lengths of 60–200 ms, there were APD₉₀ prolongation and the corresponding Ca_i overloading in the first post-pacing beats. The duration of Ca_i transient recovered to 50% (DCaT₅₀) and 90% (DCaT₉₀) in the first post-pacing beats was significantly longer than baseline. Abnormal Ca_i elevation coupled with shortened APD produced late-phase 3 EAD induced triggered activity and VF. In additional 6 preparations, the heart tissues were treated with BAPTA-AM, a calcium chelator. BAPTA-AM significantly reduced the maximal Ca_i amplitude ($26.4 \pm 3.5\%$ of the control; $p < 0.001$) and the duration of Ca_i transients in the mapped region, preventing the development of EAD and triggered activity that initiated VF.

Conclusions— I_{KATP} channel activation along with Ca_i overloading are associated with the development of late phase 3 EAD and VF. Because acute myocardial ischemia activates the I_{KATP} channel, late phase 3 EADs may be a mechanism for VF initiation during acute myocardial ischemia.

Keywords

ventricular fibrillation; early afterdepolarization; triggered activity; calcium; APD shortening

Corresponding author Shien-Fong Lin, PhD, Krannert Institute of Cardiology, Indiana University School of Medicine, 1801 N. Capitol Ave, Room E308, Indianapolis, IN 46202, Tel: (317) 962-0121, linsf@iupui.edu.

Dr. Chen reports donation of equipment for animal research from Medtronic, Inc, St. Jude Medical, Cryocath & Cyberonics. Other authors: No disclosures.

INTRODUCTION

Abbreviation of repolarization by ATP-regulated potassium channel openers (I_{KATP}), as occurs in acute myocardial ischemia, has been shown to increase ventricular vulnerability to reentry and fibrillation.^{1–3} Pinacidil is known to augment I_{KATP} channel in cardiac tissues, leading to a shortening of action potential duration (APD).^{4–7} Although previous studies have demonstrated that pinacidil facilitates the induction of ventricular fibrillation (VF) by promoting reentrant activity due to refractoriness dispersion,^{8;9} information regarding the mechanism of its arrhythmogenesis in response to the corresponding intracellular calcium (Ca_i) dynamics is largely unknown.

Ca_i exerts significant influence on many membrane ion channels and plays an important role in arrhythmogenesis.^{10–14} Elevated Ca_i may activate Na-Ca exchanger current (I_{NCX}), causing diastolic elevation of transmembrane potential (V_m). During VF, the levels of diastolic Ca_i may increase to that of systolic Ca_i , reaching levels that could trigger spontaneous sarcoplasmic reticulum (SR) calcium release.¹⁵ This raises the possibility that VF might be maintained in part by effects of Ca_i -sensitive membrane currents on action potential propagation. Burashnikov and Antzelevitch showed that Ca_i overloading contributes to the development of late phase 3 early afterdepolarization (EAD) induced triggered activity, and this mechanism may be responsible for the extrasystolic activity that reinitiates fibrillation in canine atrial tissues.¹⁶ Whether or not late phase 3 EAD is also important in the generation of ventricular arrhythmias, such as VF, is not clear. In addition, VF itself induces Ca_i overloading.¹⁷ Whether the Ca_i elevation is responsible for late phase 3 EAD and VF reinitiation remains unknown. We hypothesized that Ca_i overloading with abbreviation of APD by pinacidil may promote late phase 3 EAD and triggered activity, leading to development of spontaneous VF. To test this hypothesis, we performed simultaneous V_m and Ca_i dual optical mapping of left ventricular endocardium in isolated Langendorff-perfused rabbit hearts.

MATERIALS AND METHODS

The investigation conforms with the *Guide for the Care and Use of Laboratory Animals* published by the US National Institutes of Health (NIH Publication No. 85–23, revised 1996). The study protocol was approved by the Institutional Animal Care and Use Committee (IACUC) and followed the guidelines of the American Heart Association.

Isolated Rabbit Heart with Endocardial Exposure Preparations

New Zealand White rabbits (weight of 4 to 5 kg) of either sex were intravenously injected with 1000 units of heparin and anesthetized with ketamine (20 mg/kg) and xylazine (5 mg/kg). After a median sternotomy, the whole heart was rapidly excised and retrogradely perfused through ascending aorta with 37°C Tyrode solution (pH 7.3–7.4) equilibrated with 5% CO₂ and 95% O₂. The coronary perfusion pressure was regulated between 80 and 95 mmHg. Each isolated heart was allowed to stabilize with perfusion for about 15 minutes (equilibration period) before the following dissection and mapping protocols.

Since most previous studies were performed on the epicardium of left ventricle (LV) without elucidation of the calcium dynamics in the endocardium, we performed a dual optical mapping on the LV endocardium. We first cut open the right ventricle (RV) following procedures detailed elsewhere.¹⁸ Briefly, we cut open the right atrial (RA) free wall toward atrial septum above the right coronary artery (RCA). The distal end of the RCA was tied off to ensure continuous perfusion of the RV free wall without significant leakage. Then, a base-to-apex cut along the posterior descending artery separated the free wall from the septum on one side of the ventricle, forming an RV flap. Once the RV flap was created, the

middle portion of septum was cut off to expose LV endocardium (Fig. 1A). This preparation ensured a well-perfused endocardium with normal anatomic structures exposed in the isolated rabbit heart. There were no observations of dark areas throughout the fluorescently imaged areas, indicating nonischemic tissue preparations. ECG was recorded by two widely spaced RA-LV bipoles (RA-LV) and/or RV-LV bipoles.

Experimental Protocol

We studied 22 Langendorff-perfused isolated normal rabbit hearts with and without I_{KATP} channels opener, pinacidil (Sigma-Aldrich). We performed a dose ranging study of pinacidil level at 5, 20, 40, and 80 μM . At a low level such as 5 μM , pinacidil abbreviated APD₉₀ in the endocardium by $6.3 \pm 1.6\%$. Neither EADs nor arrhythmias were inducible in the endocardial mapped region. With the increase of pinacidil concentrations to 20 and 40 μM , higher degree of APD abbreviations and some triggered activity were observed in the endocardium. Based on the results of dose ranging study, 80 μM of pinacidil was found to be the most effective in shortening APD and inducing EADs and triggered arrhythmias. In group I (n=10), we performed simultaneous dual optical mapping of transmembrane potential (V_m) and Ca_i on LV endocardium. In group II (n=6), glass microelectrode single cell recording of transmembrane potential (TMP) was performed. In group III (n=6), we examined the effects of BAPTA-AM (20 μM ; Sigma), a calcium chelator, on late-phase 3 EAD using dual V_m and Ca_i optical mapping. For the BAPTA-AM study, the protocol was started with control, then pinacidil, followed by BAPTA-AM perfusion in the preparations. Optical and glass microelectrode measurements were made in each step to assess the effect of BAPTA-AM on arrhythmias. The ventricular endocardium was paced at a pacing cycle length (PCL) between 60 ms and 350 ms (2-ms pulse duration, 2x diastolic threshold) for 29 beats.

High Resolution, Dual Optical Mapping of V_m and Ca_i Transient

After each isolated heart was allowed to stabilize, heart tissues were double stained with V_m (RH237; Invitrogen) and Ca_i sensitive fluorescent dyes (Rhod-2 AM, 1.48 μM ; Invitrogen). After illumination by excitation laser light at 532 nm, the fluorescence was collected using two cameras (MiCAM Ultima) at 2 ms/frame with spatial resolution of $0.35 \times 0.35 \text{ mm}^2$ per pixel. The fluorescence induced by the laser illumination was obtained through a common lens, separated with a dichroic mirror (650 nm cut-off wavelength), and directed to the respective camera with additional filtering (715 nm long-pass for V_m and $580 \pm 20 \text{ nm}$ band-pass for Ca_i). Electromechanical uncoupler blebbistatin (Tocris; Ellisville, MO) was added to the perfusate at a concentration of 15 μM to eliminate motion artifacts during optical recording.¹⁹

Single Cell TMP Recordings

To confirm the optical mapping data in single myocyte, transmembrane action potential was recorded from LV endocardium using standard glass microelectrodes filled with 3M KCl, as our laboratory previously described.^{20;21} The TMP data were continuously acquired and stored for analysis using Axoscope software and an Axon Instruments Digidata 1440A acquisition system (Molecular Devices).

Statistical Analysis

Data are presented as mean \pm SD. Paired and unpaired Student's *t*-tests were used to compare the means between two groups. A *p* value of < 0.05 was considered significant.

RESULTS

Effect of Pinacidil on the Duration of Action Potential and Ca_i Transient

Fig. 1B shows optical recordings of V_m and Ca_i signals in LV endocardium with and without pinacidil. Pinacidil significantly reduced the action potential duration (APD) at 50% (APD₅₀), 90% repolarization (APD₉₀), and the corresponding duration of calcium transient (DCaT) at 50% (DCaT₅₀) in the mapped region. Fig. 1C shows the effect of pinacidil on APD and DCaT as a function of pacing cycle length (PCL) between 100 ms and 350 ms. At all PCLs, pinacidil (80 μM) reduced APD₅₀, APD₉₀, and DCaT₅₀ of LV endocardium by 34.8±7.4%, 17.4±5.7%, 14.7±3.7%, respectively, as compared to control. However, DCaT₉₀ was almost unchanged (reduced by 1.2±0.3%). For example, at PCL of 180 ms (Panel D), the APD₅₀ was reduced from 120±10 ms at baseline to 58±3 ms with pinacidil, while the APD₉₀ from 156±12 ms at baseline to 96±6 ms (p<0.0001). The corresponding DCaT₅₀ repolarization was shortened (116±8 ms at baseline to 88±7 ms; p<0.001). However, DCaT₉₀ was very similar (166±6 ms) compared to control (162±5 ms; p=NS). Due to the APD shortening by pinacidil, rapid pacing was able to capture the myocardium at PCL < 140 ms, with the minimum PCL for 1:1 capture at 60 ms.

V_m and Ca_i Dynamics of First Beat after the Cessation of Rapid Pacing

The heart preparations with and without pinacidil were paced at a PCL range from 100 to 350 ms. At the cessation of a pacing train, there was a post-pacing pause followed by spontaneous beats (Fig. 2A). At the shortest PCL (140 ms) achievable for both control and experimental groups, the pause period was significantly longer in preparations with pinacidil perfusion (795±122 ms) than control (488±27 ms; p<0.001, Fig. 2B). In the first beat following the pacing trains, both DCaT₅₀ and DCaT₉₀ were found to be lengthened by pinacidil as compared to their last paced beats (Table 1). Additionally, the amplitudes of Ca_i in the first postpacing beats were found to be increased under pinacidil (Fig. 2A, red lines). To evaluate the Ca_i amplitude change following rapid pacing, the Ca_i amplitude of first post-pacing beat was normalized to the Ca_i signal of the last paced beat. With the perfusion of pinacidil, the Ca_i level of the first post-pacing beat was increased by 35.2 ± 6.6% as compared to baseline.

The APD₉₀ of first post-pacing beat was also significantly lengthened by pinacidil (Table 1). At baseline, the APD₅₀ and APD₉₀ were not significantly increased as compared to those before pacing (APD₅₀: 140±11 ms at baseline and 148±10 ms in first post-pacing beat, p=NS; APD₉₀: 186±12 ms at baseline and 192±15 ms in first post-pacing beat, p=NS). Under pinacidil at rapid pacing (e.g. 100 ms), the APD₉₀ was increased from 92±16 ms at baseline to 186±21 ms (p<0.001) in the first post-pacing beat. The APD₅₀, however, did not show significant prolongation (38±6 ms at baseline to 39±6 ms; p=NS).

Fig. 2C shows the APD₅₀, APD₉₀, DCaT₅₀ and DCaT₉₀ values of the first post-pacing beats as function of the pacing cycle length between 100 ms and 350 ms. At baseline without pinacidil, the duration of calcium transients did not significantly increase with shortening of PCL. In contrast, with pinacidil, the DCaT₅₀ and DCaT₉₀ of first post-pacing beat were significantly (p<0.01) increased when PCL was shortened to be < 200 ms with a longer postpacing pause. It should be noted that abbreviated repolarization caused by pinacidil allowed very rapid pacing of the hearts. Thus, while the shortest possible PCL was 140 ms at baseline, evaluation of APD and DCaT at PCL < 140 ms was enabled after pinacidil perfusion.

Late-phase 3 EAD Induced by Ca_i Overloading

While there was no EADs or arrhythmias induced in control, abbreviation of APD by pinacidil perfusion and rapid pacing can lead to arrhythmia inductions. Figure 3A shows an episode of VF induced by late-phase 3 EAD. After the pause at the cessation of a pacing train at PCL of 100 ms, the first spontaneous beat was followed by a late phase 3 EAD (indicated by dashed line) and onset of VF. The EAD was the delayed repolarization that occurred before the dashed line on the V_m tracing. At the EAD initiation, the corresponding Ca_i signals remained elevated as shown in the simultaneous V_m and Ca_i optical recordings. When the V_m was depolarized (blue color in the V_m imaging), the same recording site (cross) in the Ca_i map showed high Ca_i signal (red color), indicating a persistently elevated Ca_i level. Fig. 3B shows another example of VF inductions in which Ca_i level was significantly elevated compared to that of the last paced beat (PCL: 70 ms) and remained high at the onset of late-phase 3 EAD and arrhythmia initiation. Approximately 30% of EADs in the first post-pacing beats led to VF induction where post-pacing Ca_i amplitude was at least 1.5 folds higher than that of the last paced beat. The incidence of VF induction increased at faster pacing rate. Approximately 62% EAD induced VF occurred after a pacing train at 70–100 ms, 35% at PCL of 110–130 ms, and 3% for PCL > 140 ms. This distribution is consistent with the fact that rapid pacing of the myocardium is known to induce Ca_i loading.

Transmembrane Potential Recordings Using Standard Glass Microelectrodes

We performed single cell TMP recording using glass microelectrodes in LV endocardium of six isolated rabbit hearts. Table 2 summarizes the experimental results in the single cell TMP study. The APD₉₀ of the first post-pacing beat with pinacidil was increased by 56±5.4% as compared to the last beat of the pacing train, demonstrating a repolarization prolongation. In control, the APD₉₀ was only increased by 2.3±0.7% ($p < 0.0001$). Fig. 4 shows the TMP recordings with and without pinacidil at PCL of 120 ms. To better compare the TMP morphology before and after pacing, we superimposed the last paced beat (blue traces) with the first post-pacing beat. At baseline, there was no EAD or repolarization prolongation in the first post-pacing beat (Panel A). Nor arrhythmias were induced. With pinacidil infusion, the abbreviated APD led to a prolonged post-pacing pause followed by a delayed repolarization in the first post-pacing beat (Panel B). A total of 41 episodes of repolarization prolongation were recorded in the six preparations, among which about 30% resulted in triggered activities and VF induction as shown in Panel C. The post-pacing pause duration appeared to positively correlate with the incidence of EAD and VF inductions (Panel D). At PCL of 120 ms, the pause was 182±13 ms in control. Pinacidil significantly prolonged the pause duration. When EAD was induced without VF, the pause was 356±21 ms ($p < 0.001$). When the pause was increased to 495±18 ms which might facilitate Ca_i overloading,^{16;22} EADs resulted in triggered activities and VF inductions.

BAPTA-AM

In additional six LV endocardial preparations, BAPTA-AM (20 μM), a calcium chelator,²³ was added to the Tyrode perfusate and infused for 60 minutes. The maximal Ca_i amplitude was reduced to 26.4±3.5% ($p < 0.001$) of the baseline amplitude (Fig. 5A). Neither EAD nor APD prolongation was observed in the first post-pacing beats in any of the six preparations. This is true for data obtained both from optical mapping techniques (Fig. 5B) and from single cell TMP recordings (Fig. 5C). Additionally, in none of the preparations was ventricular arrhythmia inducible after BAPTA-AM. Fig. 5D shows the effect of BAPTA-AM on the APD₉₀ prolongation of the first post-pause beat. With pinacidil only, the APD₉₀ of the first post-pacing beat was increased from 82±9 ms of last pacing beat to 148±13 ms ($p < 0.0001$), showing a late phase repolarization prolongation due to Ca_i overloading. After BAPTA-AM infusion of the same heart preparation, the APD₉₀ of the first post-pacing beat

was only slightly increased from 82 ± 9 ms of last pacing beat to 96 ± 10 ms ($p = \text{NS}$). To evaluate the Ca_i level, we normalized the Ca_i signal amplitude of the first post-pacing beat to that of the last paced beat (Fig. 5E). Before BAPTA-AM, the Ca_i level of the first post-pacing beat was increased by $35.2 \pm 6.6\%$ as compared to baseline. In contrast, after BAPTA-AM, the Ca_i increased only by $9.6 \pm 3.9\%$ ($p < 0.001$ when compared to Ca_i increase before BAPTA-AM perfusion). The duration of Ca_i transient, DCaT_{50} , of the first post-pacing beating was lengthened by approximately $125 \pm 19\%$ normalized to the last paced beat during pinacidil infusion. In contrast, the DCaT_{50} change was almost negligible after BAPTA-AM ($22 \pm 2\%$; $p < 0.0001$).

DISCUSSION

We performed simultaneous V_m and Ca_i optical mapping study of LV endocardium in isolated Langendorff-perfused rabbit hearts. Activating I_{KATP} by infusion of pinacidil at high concentration of $80 \mu\text{M}$ markedly shortened the APD in the mapped region. Abbreviation of APD allowed very rapid pacing rates of the myocardium, known to induce Ca_i loading as occurs during VF. Our study provides evidence, for the first time, in support of the hypothesis that very rapid rates of excitation with APD shortened by activation of I_{KATP} can lead to an elevation of Ca_i and prolongation of APD after pause. These changes in turn contribute to the development of late-phase 3 EAD, triggered activity, and VF induction. To the best of our knowledge, the present study is the first that not only demonstrates late-phase 3 EAD in ventricles, but also elucidates the Ca_i dynamics during late-phase 3 EADs and arrhythmia inductions by simultaneous V_m and Ca_i dual-mapping.

Late-phase 3 EAD and VF

Studies suggested that a relatively small increase in the intensity of the I_{KATP} can contribute importantly to the development of electrical inhomogeneity in the ventricles and thus to the genesis of cardiac arrhythmias.^{24–26} Pinacidil activates I_{KATP} , leading to an abbreviation of APD.⁴ The present study demonstrated a direct evidence that abbreviation of repolarization coupled with the Ca_i overload following post-pacing pause can contribute to VF induction. Our findings provided insights into a novel mechanism of ventricular arrhythmogenesis caused by late-phase 3 EAD.

The results indicated a positive relationship between the duration of post-pacing pause and the VF incidence. Approximately 30% of EADs resulted in VF inductions. The pause was significantly longer in those episodes where VFs were induced following EAD in the beats after train. Faster pacing increased the incidence of delayed repolarization and VF initiation. No endocardial reentry was observed during the onset of VF induced by late-phase 3 EADs. This is mainly because the mapping area in this study was focused on the endocardium. Phase 2 reentry is an epicardial phenomenon, for the appearance of which a prominent phase 2 must be present. A prominent phase 2 can be seen in epicardium but not in endocardium. Although no reentry was present in the mapping area, these two mechanisms are not mutually exclusive, and may both be important in the induction of VF during acute ischemia. Previous studies showed that phase 2 reentry originated on epicardial surface of the right ventricle was a trigger for VF initiation during acute ischemia in canine model.²⁷

Role of Ca_i Elevation

Our observations in the present V_m and Ca_i dual mapping study demonstrated, as discussed by Burashnikov and Antzelevitch¹⁶, that levels of Ca_i would peak during the plateau of action potential under control condition, but during the late phase of repolarization in the presence of pinacidil. The relationship between Ca_i and APD is complex and bidirectional. Ca_i determines the shape of V_m and APD through various calcium mediated ionic channels,

such as the I_{CaL} and the I_{NCX} .^{13,14} The elevated Ca_i level are restored during repolarization by the rapid reuptake of Ca_i into the SR. When the APD is shortened by pinacidil, the duration of Ca_i transient did not proportionally shorten because the Ca_i reuptake is not entirely a voltage dependent process. As a result, there was a persistent and heterogeneous Ca_i elevation after the end of action potential. The elevated Ca_i level in the first post-pacing beat could activate the electrogenic I_{NCX} which is most likely an underlying mechanisms for late-phase 3 EAD development. Additionally, the hypothesis was supported by the suppression of EADs and arrhythmia inductions after infusion of BAPTA-AM over a 60-min period. BAPTA-AM, a calcium chelator, significantly reduced the Ca_i level and prevented calcium accumulation by rapid pacing rates of excitation (Fig. 5). Consequently, no VF was inducible after BAPTA-AM infusion.

Ca_i plays an important role in controlling cardiac excitation, implying a direct coupling between Ca_i and membrane currents. Although cellular Ca_i overload plays a dominant role, it may not be the only factor responsible for EAD and arrhythmias development. Indeed, rapid pacing and pauses could lead to some degree of Ca_i overload. Our control study in the absence of pinacidil did not demonstrate EADs and arrhythmias after pacing, although strong post-pacing contractions were recorded both in controls and in the presence of pinacidil. The present study suggested that dramatic APD abbreviation and apparently strong SR Ca_i release are needed to elicit EADs and arrhythmias in the initial period after rapid pacing train.

Role of APD Shortening and Hyperpolarization

Pinacidil is known to dramatically shorten APD. In addition to APD shortening, pinacidil induced hyperpolarization, which may be responsible for longer pauses that enhanced Ca_i accumulation. Subsequent large SR calcium release in the first post-rapid-pacing beats played an important role in causing late phase 3 EADs and triggered activity. As discussed elsewhere, APD abbreviation is commonly thought to be an arrhythmogenic substrate by reducing the wavelength for reentry and promoting dispersion of repolarization and refractoriness. Our data clearly demonstrated no reentrant activities in endocardium, thereby we believe for the first time that dramatic APD shortening coupled with a pause-induced strong Ca_i overload may contribute to ventricular arrhythmogenesis by allowing for the development of late-phase 3 EAD induced triggered activity.

Clinical Implications

The results of the present study have significant clinical implications for recurrent spontaneous VF during cardiopulmonary resuscitation and in short-QT syndrome. In approximately 50% of the patients who receive defibrillation shocks during cardiopulmonary resuscitation, initial successful defibrillation is followed by recurrent spontaneous VF.²⁸ Recurrent spontaneous VF is associated with high morbidity and mortality, and may lead to arrhythmic death in spite of an ICD.²⁹⁻³² A possible mechanism of spontaneous VF is that the cessation of coronary circulation during VF may result in acute myocardial ischemia, which activates I_{KATP} and shortens the APD. In addition to causing ischemia, VF also results in Ca_i accumulation. A combination of short APD and Ca_i accumulation may promote late phase 3 EAD, triggered activities and VF. Short-QT syndrome³³ is a rare genetic disorder characterized by short-QT interval but normal duration of mechanical systole,³⁴ suggesting short APD and normal Ca_i transient. The present study shows that a combination of short APD and prolonged DCaT can lead to spontaneous VF through late-phase 3 EAD. A clinical implication of this present study is that late phase 3 EAD is responsible for recurrent spontaneous VF during cardiopulmonary resuscitation and patients with short-QT syndrome. Prevention of late phase 3 EAD may reduce the incidence of recurrent VF in these patients.

Acknowledgments

This work was supported in part by National Institutes of Health [P01 HL78931, R01s HL78932, 66389, 71140], a Medtronic-Zipes Endowment and an AHA Established Investigator Award [#0540093N].

Reference List

1. Padrini R, Bova S, Cargnelli G, Piovan D, Ferrari M. Effects of pinacidil on guinea-pig isolated perfused heart with particular reference to the proarrhythmic effect. *Br J Pharmacol*. 1992; 105:715–719. [PubMed: 1628158]
2. Uchida T, Yashima M, Gotoh M, Qu Z, Garfinkel A, Weiss JN, Fishbein MC, Mandel WJ, Chen P-S, Karagueuzian HS. Mechanism of acceleration of functional reentry in the ventricle: effects of ATP-sensitive potassium channel opener. *Circulation*. 1999; 99:704–712. [PubMed: 9950670]
3. Coromilas J, Costeas C, Deruyter B, Dillon SM, Peters NS, Wit AL. Effects of pinacidil on electrophysiological properties of epicardial border zone of healing canine infarcts: possible effects of K(ATP) channel activation. *Circulation*. 2002; 105:2309–2317. [PubMed: 12010915]
4. Arena JP, Kass RS. Enhancement of potassium-sensitive current in heart cells by pinacidil. Evidence for modulation of the ATP-sensitive potassium channel. *Circ Res*. 1989; 65:436–445. [PubMed: 2752550]
5. Traverse JH, Chen Y, Hou M, Li Y, Bache RJ. Effect of K⁺ATP channel and adenosine receptor blockade during rest and exercise in congestive heart failure. *Circ Res*. 2007; 100:1643–1649. [PubMed: 17478726]
6. Lee TM, Lin MS, Chang NC. Effect of ATP-sensitive potassium channel agonists on ventricular remodeling in healed rat infarcts. *J Am Coll Cardiol*. 2008; 51:1309–1318. [PubMed: 18371564]
7. Wu S, Hayashi H, Lin SF, Chen PS. Action Potential Duration and QT Interval During Pinacidil Infusion in Isolated Rabbit Hearts. *J Cardiovasc Electrophysiol*. 2005; 16:872–878. [PubMed: 16101630]
8. Chi L, Uprichard ACG, Lucchesi BR. Profibrillatory actions of pinacidil in a conscious canine model of sudden coronary death. *J Cardiovasc Pharmacol*. 1990; 15:452–464. [PubMed: 1691370]
9. Di Diego JM, Antzelevitch C. Pinacidil-induced electrical heterogeneity and extrasystolic activity in canine ventricular tissues. Does activation of ATP-regulated potassium current promote phase 2 reentry? *Circulation*. 1993; 88:1177–1189. [PubMed: 7689041]
10. Merillat JC, Lakatta EG, Hano O, Guarnieri T. Role of calcium and the calcium channel in the initiation and maintenance of ventricular fibrillation. *Circ Res*. 1990; 67:1115–1123. [PubMed: 2171799]
11. Goldhaber JJ, Xie LH, Duong T, Motter C, Khuu K, Weiss JN. Action potential duration restitution and alternans in rabbit ventricular myocytes: the key role of intracellular calcium cycling. *Circ Res*. 2005; 96:459–466. [PubMed: 15662034]
12. Omichi C, Lamp ST, Lin SF, Yang J, Baher A, Zhou S, Attin M, Lee MH, Karagueuzian HS, Kogan B, Qu Z, Garfinkel A, Chen PS, Weiss JN. Intracellular Ca dynamics in ventricular fibrillation. *Am J Physiol Heart Circ Physiol*. 2004; 286:H1836–H1844. [PubMed: 14704235]
13. Bers DM. Calcium fluxes involved in control of cardiac myocyte contraction. *Circ Res*. 2000; 87:275–281. [PubMed: 10948060]
14. Choi BR, Salama G. Simultaneous maps of optical action potentials and calcium transients in guinea-pig hearts: mechanisms underlying concordant alternans. *J Physiol*. 2000; 529 (Pt 1):171–188. [PubMed: 11080260]
15. Stefenelli T, Wikman-Coffelt J, Wu ST, Parmley WW. Intracellular calcium during pacing-induced ventricular fibrillation. Effects of lidocaine. *J Electrocardiol*. 1992; 25:221–228. [PubMed: 1645062]
16. Burashnikov A, Antzelevitch C. Reinduction of atrial fibrillation immediately after termination of the arrhythmia is mediated by late phase 3 early afterdepolarization-induced triggered activity. *Circulation*. 2003; 107:2355–2360. [PubMed: 12695296]

17. Zaugg CE, Wu ST, Barbosa V, Buser PT, Wikman-Coffelt J, Parmley WW, Lee RJ. Ventricular fibrillation-induced intracellular Ca²⁺ overload causes failed electrical defibrillation and post-shock reinitiation of fibrillation. *J Moll Cell Cardiol.* 1998; 30:2183–2192.
18. Tang L, Hwang GS, Hayashi H, Song J, Ogawa M, Kobayashi K, Joung B, Karagueuzian HS, Chen PS, Lin SF. Intracellular calcium dynamics at the core of endocardial stationary spiral waves in Langendorff-perfused rabbit hearts. *Am J Physiol Heart Circ Physiol.* 2008; 295:H297–H304. [PubMed: 18487432]
19. Fedorov VV, Lozinsky IT, Sosunov EA, Anyukhovskiy EP, Rosen MR, Balke CW, Efimov IR. Application of blebbistatin as an excitation-contraction uncoupler for electrophysiologic study of rat and rabbit hearts. *Heart Rhythm.* 2007; 4:619–626. [PubMed: 17467631]
20. Ikeda T, Yashima M, Uchida T, Hough D, Fishbein MC, Mandel WJ, Chen P-S, Karagueuzian HS. Attachment of meandering reentrant wave fronts to anatomic obstacles in the atrium. Role of the obstacle size. *Circ Res.* 1997; 81:753–764. [PubMed: 9351449]
21. Kim Y-H, Yashima M, Wu T-J, Doshi R, Chen P-S, Karagueuzian HS. Mechanism of procainamide-induced prevention of spontaneous wave break during ventricular fibrillation. Insight into the maintenance of fibrillation wave fronts. *Circulation.* 1999; 100:666–674. [PubMed: 10441106]
22. Patterson E, Lazzara R, Szabo B, Liu H, Tang D, Li YH, Scherlag BJ, Po SS. Sodiumcalcium exchange initiated by the Ca²⁺ transient: an arrhythmia trigger within pulmonary veins. *J Am Coll Cardiol.* 2006; 47:1196–1206. [PubMed: 16545652]
23. Tsien RY. A non-disruptive technique for loading calcium buffers and indicators into cells. *Nature.* 1981; 290:527–528. [PubMed: 7219539]
24. Antzelevitch C, Sicouri S, Litovsky SH, Lukas A, Krishnan SC, Di Diego JM, Gintant GA, Liu D-W. Heterogeneity within the ventricular wall. Electrophysiology and pharmacology of epicardial, endocardial, and M cells. *Circ Res.* 1991; 69:1427–1449. [PubMed: 1659499]
25. Smeets JL, Alessie MA, Lammers WJ, Bonke FI, Hollen J. The wavelength of the cardiac impulse and reentrant arrhythmias in isolated rabbit atrium. The role of heart rate, autonomic transmitters, temperature, and potassium. *Circ Res.* 1986; 58:96–108. [PubMed: 3943157]
26. Yan GX, Antzelevitch C. Cellular basis for the Brugada syndrome and other mechanisms of arrhythmogenesis associated with ST-segment elevation. *Circulation.* 1999; 100:1660–1666. [PubMed: 10517739]
27. Yan GX, Joshi A, Guo D, Hlaing T, Martin J, Xu X, Kowey PR. Phase 2 reentry as a trigger to initiate ventricular fibrillation during early acute myocardial ischemia. *Circulation.* 2004; 110:1036–1041. [PubMed: 15302777]
28. Hess EP, White RD. Out-of-hospital cardiac arrest in patients with cardiac amyloidosis: presenting rhythms, management and outcomes in four patients. *Resuscitation.* 2004; 60:105–111. [PubMed: 14987790]
29. Ohgo T, Okamura H, Noda T, Satomi K, Suyama K, Kurita T, Aihara N, Kamakura S, Ohe T, Shimizu W. Acute and chronic management in patients with Brugada syndrome associated with electrical storm of ventricular fibrillation. *Heart Rhythm.* 2007; 4:695–700. [PubMed: 17556186]
30. Exner DV, Pinski SL, Wyse DG, Renfroe EG, Follmann D, Gold M, Beckman KJ, Coromilas J, Lancaster S, Hallstrom AP. Electrical storm presages nonsudden death: the antiarrhythmics versus implantable defibrillators (AVID) trial. *Circulation.* 2001; 103:2066–2071. [PubMed: 11319196]
31. Maury P, Couderc P, Delay M, Boveda S, Brugada J. Electrical storm in Brugada syndrome successfully treated using isoprenaline. *Europace.* 2004; 6:130–133. [PubMed: 15018871]
32. Nademanee K, Taylor R, Bailey WE, Rieders DE, Kosar EM. Treating electrical storm: sympathetic blockade versus advanced cardiac life support-guided therapy. *Circulation.* 2000; 102:742–747. [PubMed: 10942741]
33. Gaita F, Giustetto C, Bianchi F, Wolpert C, Schimpf R, Riccardi R, Grossi S, Richiardi E, Borggrefe M. Short QT Syndrome: a familial cause of sudden death. *Circulation.* 2003; 108:965–970. [PubMed: 12925462]
34. Schimpf R, Antzelevitch C, Haghi D, Giustetto C, Pizzuti A, Gaita F, Veltmann C, Wolpert C, Borggrefe M. Electromechanical coupling in patients with the short QT syndrome: further insights

into the mechanoelectrical hypothesis of the U wave. *Heart Rhythm*. 2008; 5:241–245. [PubMed: 18242547]

\$watermark-text

\$watermark-text

\$watermark-text

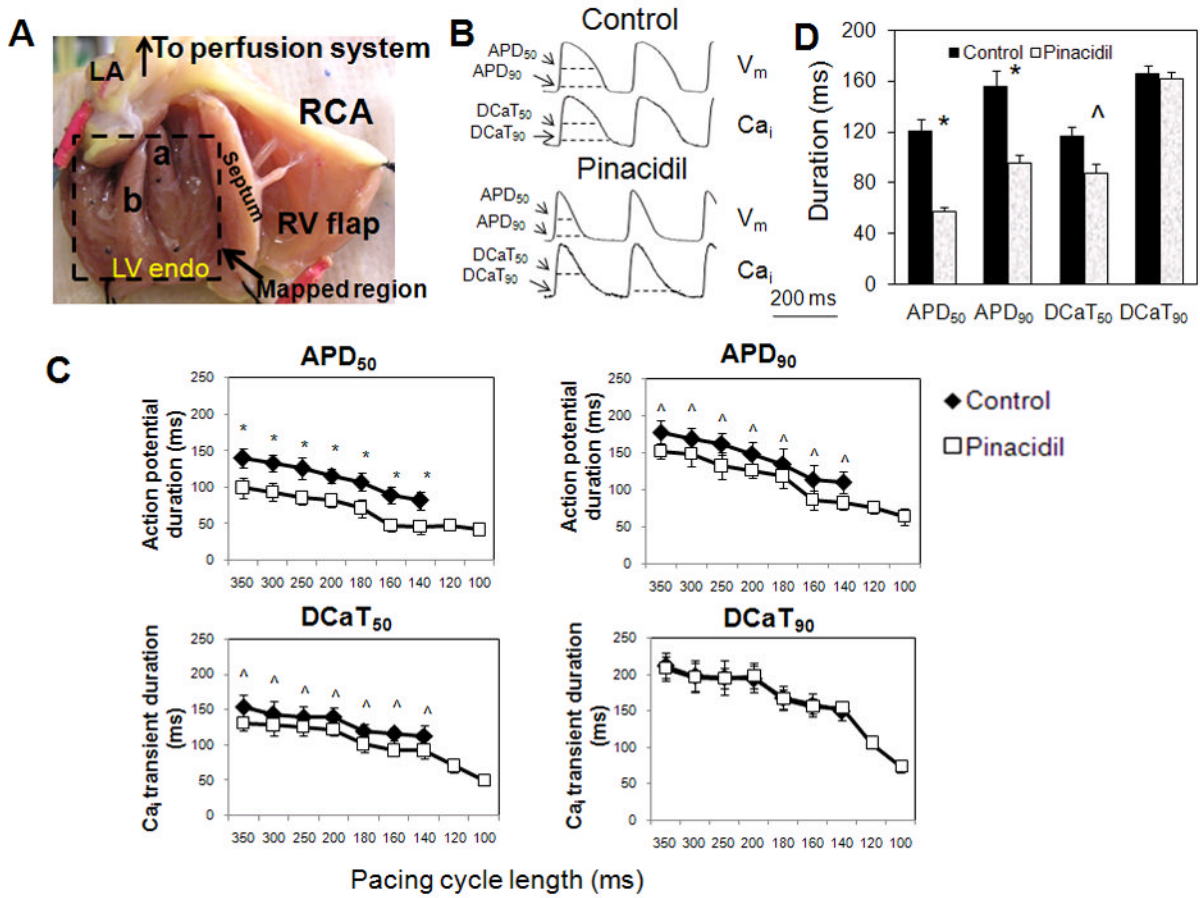


Figure 1.
 A: Cut-open LV preparation in Langendorff-perfused isolated rabbit hearts. LA: left atrium; RCA: right coronary artery; LV endo: left ventricle endocardium; RV: right ventricle; a: anterior papillary muscle; b: posterior papillary muscle. B: Optical recording traces of V_m and Ca_i of LV endocardium at pacing cycle length (PCL) of 250 ms. APD_{50} : action potential duration measured to 50% repolarization; APD_{90} : action potential duration measured to 90% repolarization; $DCaT_{50}$: duration of Ca_i transient measured to 50% repolarization; $DCaT_{90}$: duration of Ca_i transient measured to 90% repolarization. C: Effects of pinacidil on APD_{50} , APD_{90} , $DCaT_{50}$, and $DCaT_{90}$ as a function of pacing cycle length between 100 and 350 ms. D: Comparison of the APD and DCaT in control and pinacidil at PCL of 180 ms. * $p < 0.0001$; ^ $p < 0.001$

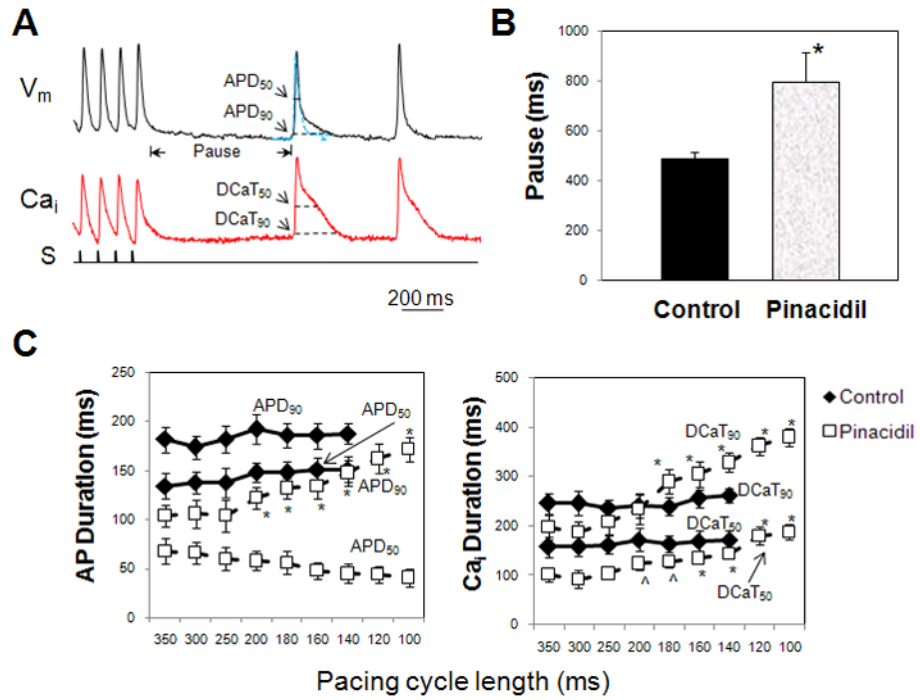


Figure 2.
 A: Optical signals of V_m and Ca_i of beats following pause after pacing with pinacidil. Rapid pacing with pinacidil produced an APD prolongation of first post-pacing beat. Blue traces indicate the morphology of action potentials of the last beat in the pacing train. S, pacing stimulus. B: Pinacidil induced a longer pause following pacing train. $*p < 0.001$. C: Effects of pinacidil on APD_{50} , APD_{90} , $DCaT_{50}$, and $DCaT_{90}$ of first post-pacing beat when PCL decreased from 350 to 100 ms. Rapid pacing under pinacidil produced a prolongation of APD_{90} and increase of $DCaT_{50}$ and $DCaT_{90}$. $*p < 0.001$; $^{\wedge}p < 0.01$ as compared to pacing cycle length greater than 250 ms.

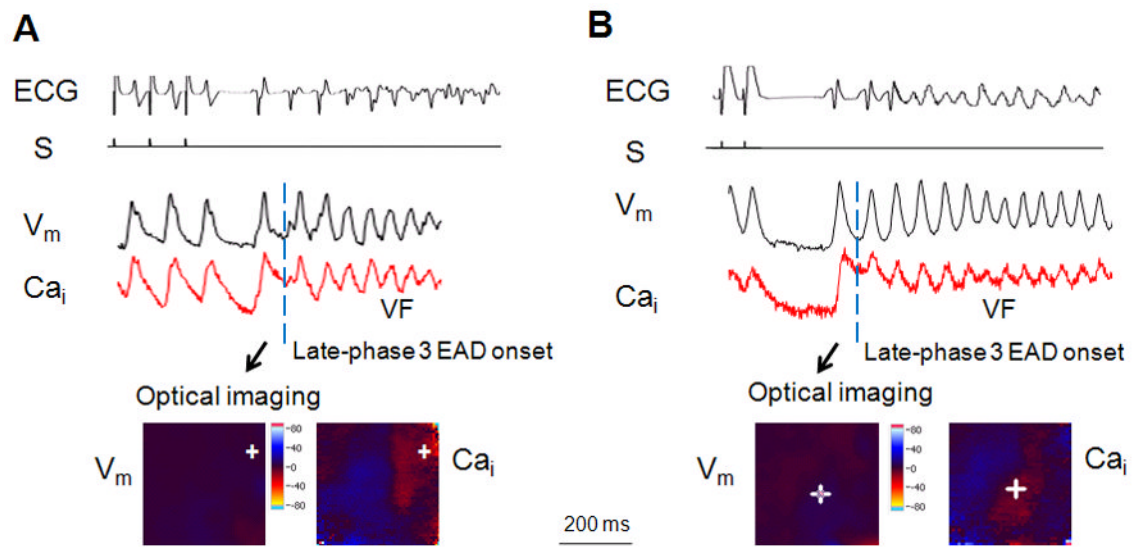


Figure 3.

A: Typical V_m and Ca_i signals of late-phase 3 EAD induced triggered activity and ventricular fibrillation. The late phase 3 EAD is the delayed repolarization that occurred before the dashed line on the V_m tracing. PCL: 90 ms. S: pacing stimulus. B: V_m and Ca_i recordings for VF onset induced by EADs after post-pacing pause. PCL at 70 ms. Cross indicates the origin of the EAD in the mapped region.

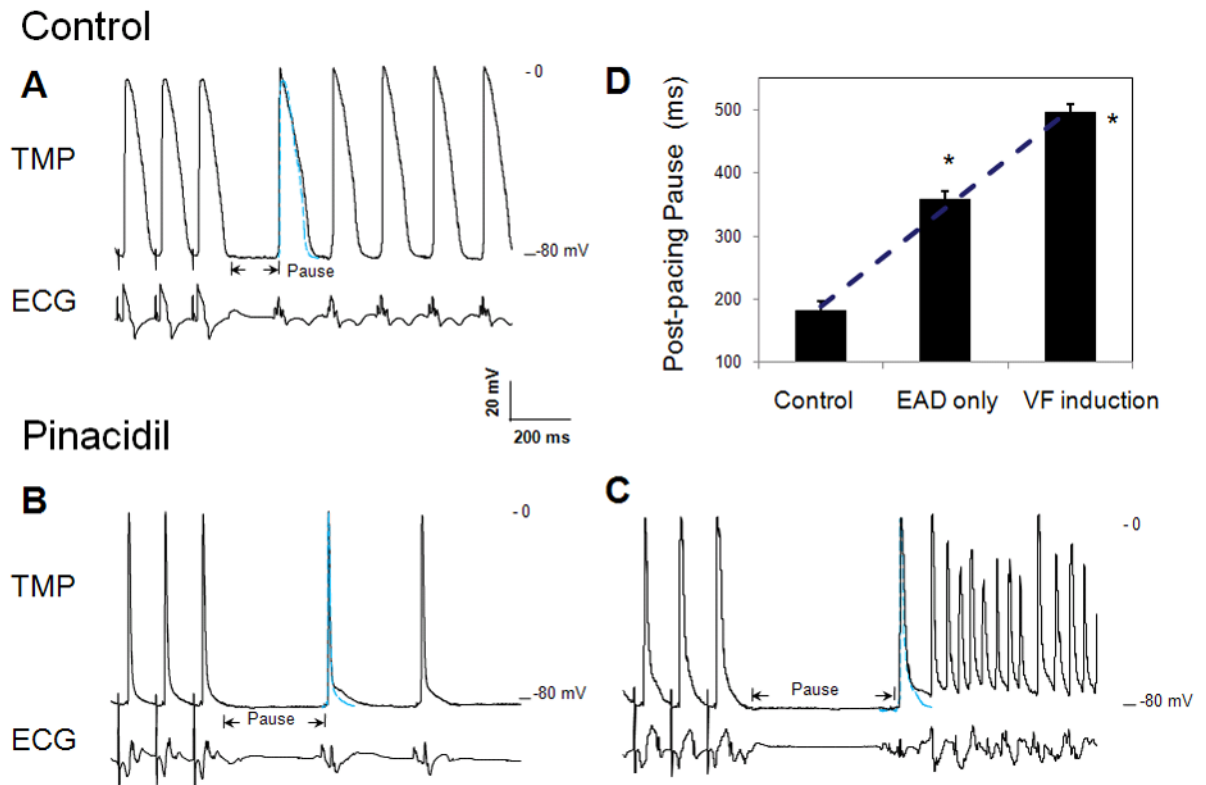


Figure 4.

Glass microelectrode recordings of transmembrane potential (TMP) of single myocyte in LV endocardium of isolated rabbit hearts. Blue traces indicate the TMP recording of the last paced beat in the train. A: control study. B and C: pinacidil infusion to produce APD₉₀ prolongation in first post-pacing beat (B) and late-phase 3 EAD induced triggered activities and VF (C). PCL at 120 ms. D: comparison of the post-pacing pause duration in control, EAD, and VF induction. * $p < 0.0001$

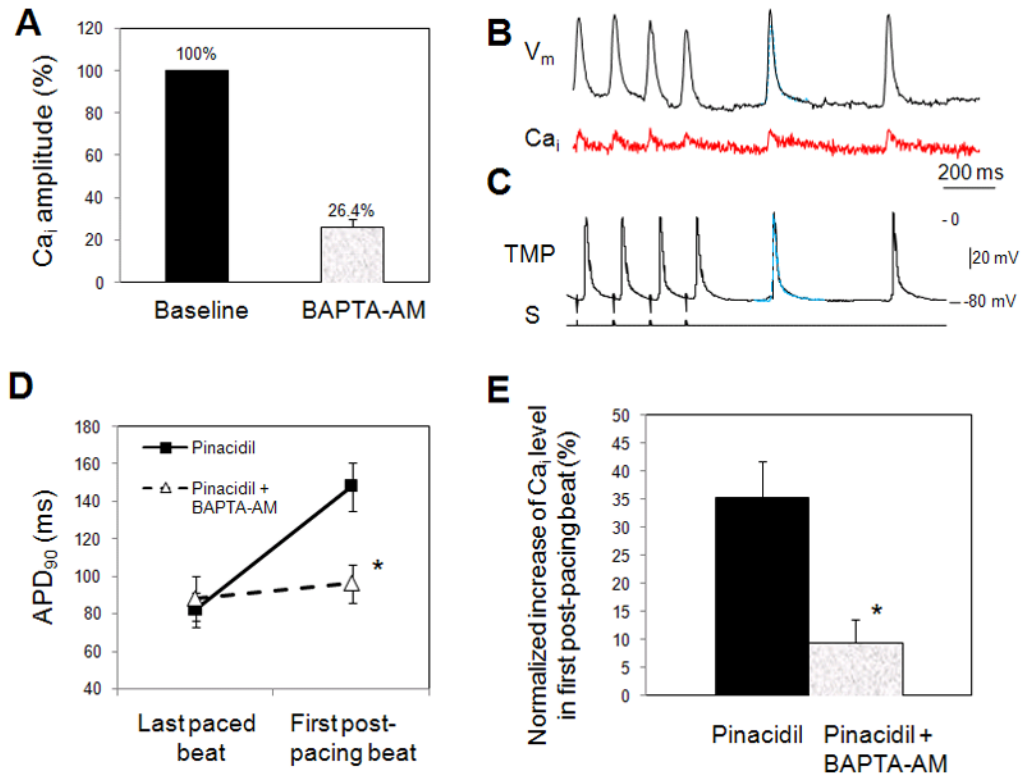


Figure 5.

A: BAPTA-AM significantly reduced the maximal Ca_i amplitudes normalized to baseline. B: V_m and Ca_i optical signal recordings after BAPTA-AM perfusion showed no APD prolongation in first post-pacing beats. Blue traces indicate the action potential recording of the last paced beats in the train. C: Glass microelectrode TMP recording in BAPTA-AM study. D: Effect of BAPTA-AM on post-rapid pacing APD₉₀. Optical imaging data (n=6). E: BAPTA-AM significantly reduced the corresponding Ca_i increase in first post-pacing beat. The Ca_i increase magnitude was normalized to the Ca_i level in last pacing beat. * $p < 0.001$.

Table 1

Comparison of post-pacing beats' action potential duration (APD), Ca_i duration (DCaT) and amplitude to those of the last paced beats in heart preparation of control (n=10), under pinacidil (n=10), and after BAPTA-AM infusion (n=6).

	Control	Pinacidil	BAPTA-AM
Post-pacing Pause	488±27 ms	795±122 ms *	320±22 ms §
Post-pause APD₅₀ prolongation	5.7±1.1%	2.6±0.3%	1.6±0.5%
Post-pause APD₉₀ prolongation	3.2±0.8%	102±18% *	2.1±0.4% §
Post-pause DCaT₅₀ prolongation	8±1.4%	125±19% *	22±2% §
Post-pause Ca_i Amplitude Increase	--	35.2±6.6% *	9.6±3.9% §
EAD	None	In all 10 preparations	None
VF induction	None	In all 10 preparations	None

* $p < 0.001$ between control and pinacidil group;

§ $p < 0.001$ between pinacidil and BAPTA-AM group

Watermark-text

Watermark-text

Watermark-text

Table 2

Summary of the post-pacing pause, post-pacing APD, early afterdepolarization (EAD) and ventricular fibrillation (VF) inductions in glass microelectrode study (n=6; PCL: 120 ms).

#	Post-pacing Pause (ms)		Post-pause APD ₉₀ prolongation (%)		No. of EAD episodes		No. of VF episodes		
	Control	Pinacidil + EAD	Pinacidil + VF	Control	Pinacidil	Control	Pinacidil	Control	Pinacidil
1	160	340	480	2.2	53.1	--	8	--	2
2	180	330	520	1.5	47.3	--	5	--	1
3	176	345	473	2.6	61.5	--	7	--	3
4	193	367	498	3.2	54.6	--	6	--	1
5	182	380	486	2.8	59.2	--	8	--	3
6	198	376	510	1.8	60.4	--	7	--	2
Mean	182±13	356±21 §	495±18 §	2.3±0.7	56±5.4 §	None	Total: 41	None	Total: 12

§ $p < 0.001$